



OPEN ACCESS

EDITED BY

Magdalena Jasinska-Stroschein,
Medical University of Lodz, Poland

REVIEWED BY

Li Peng,
Shanxi Agricultural University, China
Muhammad Tahir Ul Qamar,
Government College University, Faisalabad,
Pakistan

*CORRESPONDENCE

Yonghong Zhang,
✉ zhyvonne26@cqmu.edu.cn

RECEIVED 07 May 2024

ACCEPTED 13 September 2024

PUBLISHED 01 October 2024

CITATION

Chen X, Zhou B, Jiang X, Zhong H, You A, Zou T,
Zhou C, Liu X and Zhang Y (2024) Drug
repurposing to tackle parainfluenza 3 based on
multi-similarities and network
proximity analysis.
Front. Pharmacol. 15:1428925.
doi: 10.3389/fphar.2024.1428925

COPYRIGHT

© 2024 Chen, Zhou, Jiang, Zhong, You, Zou,
Zhou, Liu and Zhang. This is an open-access
article distributed under the terms of the
[Creative Commons Attribution License \(CC BY\)](https://creativecommons.org/licenses/by/4.0/).
The use, distribution or reproduction in other
forums is permitted, provided the original
author(s) and the copyright owner(s) are
credited and that the original publication in this
journal is cited, in accordance with accepted
academic practice. No use, distribution or
reproduction is permitted which does not
comply with these terms.

Drug repurposing to tackle parainfluenza 3 based on multi-similarities and network proximity analysis

Xinyue Chen¹, Bo Zhou^{1,2}, Xinyi Jiang¹, Huayu Zhong¹,
Aijing You³, Taiyan Zou^{1,4,5}, Chengcheng Zhou¹, Xiaoxiao Liu¹
and Yonghong Zhang^{1,4,5*}

¹Chongqing Key Research Laboratory for Drug Metabolism, College of Pharmacy, Chongqing Medical University, Chongqing, China, ²Department of Pharmacy, Children's Hospital of Chongqing Medical University, Chongqing, China, ³The Second Clinical College of Chongqing Medical University, Chongqing, China, ⁴Medical Data Science Academy, College of Medical Informatics, Chongqing Medical University, Chongqing, China, ⁵Chongqing Engineering Research Center for Clinical Big-Data and Drug Evaluation, Chongqing Medical University, Chongqing, China

Given that there is currently no clinically approved drug or vaccine for parainfluenza 3 (PIV3), we applied a drug repurposing method based on disease similarity and chemical similarity to screen 2,585 clinically approved chemical drugs using PIV3 potential drugs BCX-2798 and zanamivir as our controls. Twelve candidate drugs were obtained after being screened with good disease similarity and chemical similarity ($S > 0.50$, $T > 0.56$). When docking them with the PIV3 target protein, hemagglutinin-neuraminidase (HN), only oseltamivir was docked with a better score than BCX-2798, which indicates that oseltamivir has an inhibitory effect on PIV3. After the distance (Z_{dc}) between the drug target of 14 drugs and the PIV3 disease target was measured by the network proximity method based on the PIV3 disease module, it was found that the Z_{dc} values of amikacin, oseltamivir, ribavirin, and streptomycin were less than those of the control. Thus, oseltamivir is the best potential drug because it met all the above screening requirements. Additionally, to explore whether oseltamivir binds to HN stably, molecular dynamics simulation of the binding of oseltamivir to HN was carried out, and the results showed that the $RMSD$ value of the complex tended to be stable within 100 ns, and the binding free energy of the complex was low (-10.60 kcal/mol). It was proved that oseltamivir screened by our drug repurposing method had the potential feasibility of treating PIV3.

KEYWORDS

parainfluenza 3, drug repurposing, chemical similarity, disease similarity, network proximity

Introduction

There is no specific antiviral treatment for parainfluenza (PIV) illness. Most people with PIV illness will recover on their own. However, PIVs can also cause more serious illnesses in children and adults older than 65 years, including bronchitis, bronchiolitis, and pneumonia (Moscona, 2005; Schmidt et al., 2011). Among PIVs, parainfluenza 3 (PIV3) is the most prevalent subtype, and it is not only a most common cause of acute respiratory infections in infants, but it also causes severe respiratory symptoms in older adults,

immunocompromised patients, and transplant recipients (Branche and Falsey, 2016). Despite causing serious health problems, there is currently no clinically approved drug or vaccine for PIV3 (Contreras et al., 2021; Rafeek et al., 2021). PIV3 infects its target cells through the coordinated action of the hemagglutinin-neuraminidase receptor-binding protein (HN) and the fusion envelope glycoprotein, which together comprise the molecular fusion machinery (Palmer et al., 2014; Van Den Bergh et al., 2022). Peptide-fusion protein inhibitors that target the fusion envelope glycoprotein are challenging to utilize in clinical settings because of limitations such as high manufacturing costs, low oral bioavailability, and severe injection site reactions caused by the immunogenicity of virus-derived peptides (Aggarwal and Plemper, 2020). Current preclinical development and clinical trials for treating PIV3 primarily focus on inhibitors that target the HN protein (Chibanga et al., 2019; Rota et al., 2023).

At present, the common PIV3 drug research and development is carried out on HN inhibitors using virtual screening by molecular docking. Molecular docking is one of the most commonly used strategies in structure-based drug design (Parihar et al., 2022; Tayubi and Madar, 2023) and has been widely employed in the development of anti-PIV3 drugs (Indumathi et al., 2019; Bhasin et al., 2022). Zanamivir successfully docked with HN, and it has been proven to have anti-PIV3 effects *in vitro*, but is not suitable for clinical use due to its relatively high IC50 (Bailly et al., 2016). In the current clinical studies of PIV3, BCX-2798 has been shown to inhibit HN in mouse models, and this research has only recently progressed to the clinical stage. Further trials are necessary before it can be practically applied (Alyмова et al., 2005). However, these classical screening methods often ignore the progression of the disease, and drug safety also needs to be fully assessed.

Recently, drug repurposing strategies, with the advantage of drug safety, have become strong approaches to the research and development of antiviral drugs (Kumar et al., 2021; Sonkar et al., 2021). The disease similarity and chemical similarity were calculated to uncover associations between diseases and drugs for use in drug repurposing (Li et al., 2018; Yin et al., 2023; Pushpakom et al., 2019). Interestingly, zanamivir and BCX-2798 are both derived from Neu5Ac2en, the neuraminidase (NA) inhibitor (Alyмова et al., 2004). Their ability to inhibit PIV3 suggests that structurally similar compounds often share similar physicochemical properties and biological activities (Durai et al., 2020). Apart from structure-based virtual screening (Khan et al., 2023), the network-based drug-disease proximity method that uncovers the relationship between drug targets and disease modules is widely used (Yildirim et al., 2007; Zhou et al., 2020), and it is utilized not only for predicting the potential side effects but also for repurposing approved drugs for new indications (Guney et al., 2016; Wang et al., 2021; Xi et al., 2023).

Therefore, this research focuses on the following: 1) multi-similarity methods to understand the intrinsic link between diseases and drugs, 2) the structural characteristic link of potential drugs, and 3) the network proximity of disease targets and drug targets to understand drugs related to the occurrence and onset of diseases. We combined disease and chemical similarity methods to screen candidate drugs against PIV3. Molecular docking and network proximity methods were used to identify the best anti-PIV3 drug. Finally, the binding ability and stability of candidate

drugs and key disease targets in a dynamic environment were evaluated using molecular dynamics simulation.

Methods

Our approach involves collecting data, calculating disease similarity to PIV3, and assessing chemical similarity to potential existing drugs for PIV3. We further screen through molecular docking and assess network proximity between the drug and PIV3. Finally, we conduct molecular dynamics simulations and calculate the binding free energy. The workflow is shown in Figure 1.

Data collection

The Medical Subject Headings (MeSH) for PIV3 were obtained from <https://nlmpubs.nlm.nih.gov/projects/mesh/2022/meshtrees/> and were used to calculate the disease similarity of PIV to all other diseases in the MeSH database that contain Medical Subject Headings. We obtained the approved drugs (molecular weight <500) from the DrugBank database (<https://go.drugbank.com>) as candidate drugs for drug repurposing. Zanamivir and BCX-2798 (potential therapeutic drugs for PIV3) were considered two controls.

Disease targets associated with PIV3 were obtained by using “*parainfluenza*” as a search term from GeneCards (<https://www.genecards.org/>), OMIM (<https://www.omim.org/>), and DisGeNET (<https://www.disgenet.org/>), excluding non-coding RNA proteins. The drug targets were sourced from the DrugBank database and DGIdb (<https://dgidb.org>). All data were downloaded on 26 March 2024. Disease genes and drug targets were sorted out with the same format in UniProt using Python 3.9.

Multi-similarity analysis

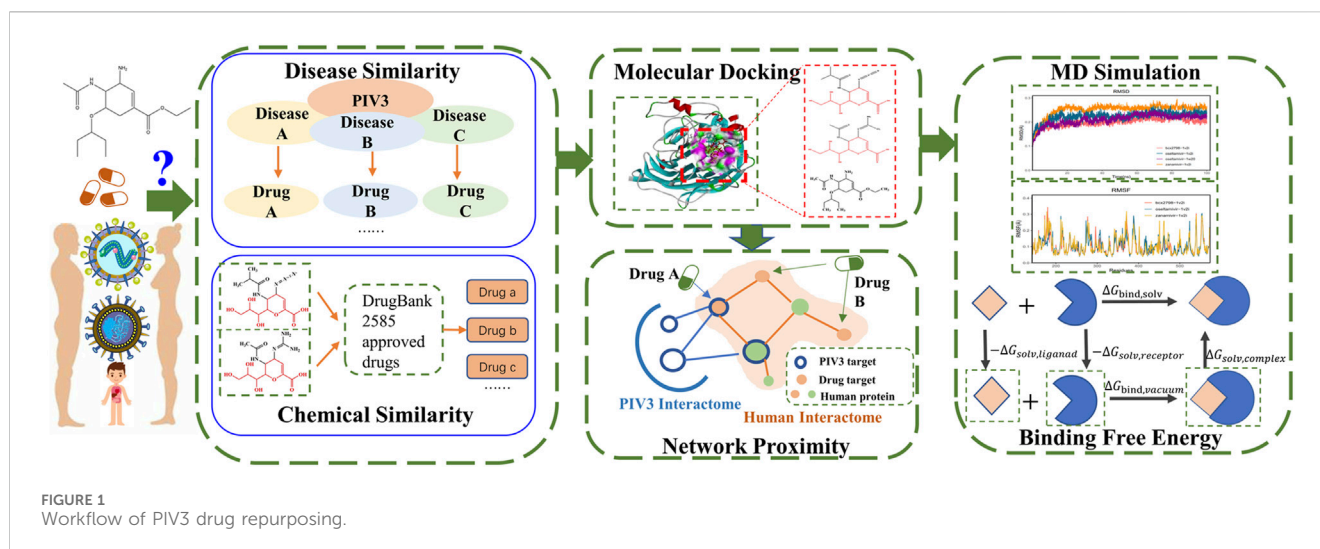
Multi-similarity analysis, including disease therapy similarity and drug chemical similarity, was used to virtually screen all candidate drugs. The disease therapy similarity is calculated based on the directed acyclic graph (DAG), which is constructed using grid descriptors (Wang et al., 2007). The disease PIV3 are represented by $DAG_{(H)} = \{T_H, E_H\}$, where T_H is the set of ancestor nodes containing node PIV3 and E_H represents the set of edges from the parent node to the child node. In $DAG_{(H)}$, the contribution of a certain node N to PIV3 ($SV_H(n)$) is calculated as Equation 1:

$$SV_H(n) = \begin{cases} 1 & \text{if } n = H \\ \max\{\Delta * SV_H(n') | n' \in \text{children of } n\} & \text{if } n \neq H \end{cases} \quad (1)$$

The semantic similarity of PIV3 and disease A ($S_{(H,A)}$) is calculated by Equation 2. If $S_{(H,A)} > 0.5$, it indicates that there is a good similarity between these two diseases.

$$S_{(H,A)} = \frac{\sum_{n \in N(H) \cap N(A)} (SV_H(n) + SV_H(A))}{SV(H) + SV(A)} \quad (2)$$

The Tanimoto coefficient (T) was calculated to assess the chemical similarity of all drugs. After the MACCS fingerprints of



all drugs described by PaDEL (Yap, 2011), T is calculated using Equation 3:

$$T = \frac{c}{a + b - c} \quad (3)$$

where a and b are the numbers of MACCS fingerprint bits of drug A and B, respectively, and c is the number of fingerprint bits that two drugs have the same value on the MACCS fingerprint bits. If one drug has bigger T , the drug is a potential candidate.

The drugs obtained through the multi-similarity method are the initial candidates for the next round of screening.

Molecular docking

After the candidates were screened by multi-similarity analysis, we employed molecular docking to assess the docking and interaction between the screened drugs and the key target HN (PDB ID: 1V2I) (Indumathi et al., 2019). We utilized a literature-based method to identify the binding sites due to the absence of binding ligands in the original PDB structure. The key amino acids ARG192, ASP216, GLU409, ARG424, ARG502, TYR530, and GLU549 were designated as active sites (Lawrence et al., 2004; Mizuta et al., 2014; Bhasin et al., 2022). Molecular docking analyses were conducted on the selected candidates and two controls with HN using Discovery Studio 2019 (DS 2019).

Network proximity analysis

Meanwhile, the network proximity calculation will be performed to assess the shortest path lengths between the candidate drug targets and PIV3 disease module (Wang et al., 2022; Tang et al., 2023). This evaluation will determine if the candidate drugs have the potential to treat PIV3.

PIV3 disease targets were distributed throughout the protein-protein-interaction (PPI) network (Menche et al., 2015; Dai et al., 2020), forming the PIV3 disease module and constructing the largest connected component (LCC) within the PIV3 disease

module. The shortest path length (d_c , Equation 4) of the PIV3 disease target set (V) and drug target set (T) is as follows:

$$d_c(V, T) = \frac{1}{|T|} \sum_{t \in T} \min_{v \in V} d(v, t) \quad (4)$$

Using the average $\mu_d(V, T)$ and standard deviation $\sigma_d(V, T)$ of the reference distribution between randomly selected protein groups, the calculated distance is converted into the average relative distance between drugs and PIV3 diseases. Equation 5 is for calculating the relative average shortest distance between V and T . If $Z_{dc} < 0$, which means that the distance between the test drug and the PIV3 disease module is less than the value of the reference distance, then the test drug is a potential candidate for anti-PIV3 (Morselli Gysi et al., 2021).

$$Z_{dc} = \frac{dc - \mu_{dc}(V, T)}{\sigma_{dc}(V, T)} \quad (5)$$

Molecular dynamics simulation

After completing the aforementioned screening methods, we identified drugs that met all the screening requirements and conducted molecular dynamics (MD) simulations of the drugs and HN complexes using GROMACS 2022.3.

Our simulation utilized the CHARMM36 force field and TIP3P solvent (Nayar et al., 2011), with the addition of a 0.15 mol/L NaCl solution to mimic physiological conditions. The steepest descent method was chosen for energy minimization (Koulgi et al., 2021). To replicate a physiological environment, a Langevin thermostat with a pressure of 1 atm and a temperature of 310 K was applied. The particle mesh Ewald (PME) algorithm was employed for calculating long-range interactions (Darden et al., 1993; Gu et al., 2011). Moreover, the simulation employed a step size of 2 fs/step, with a total of 50,000,000 steps, resulting in a simulating duration of 100 ns. Post-simulation, an analysis was conducted on the root-mean-square deviation (RMSD), root-mean-square fluctuation (RMSF), and radius of gyration (RG) of the complex.

TABLE 1 Results of drug repurposing.

No.	Drug	<i>T</i> (zanamivir)	<i>T</i> (BCX-2798)	<i>CE</i> (kcal/mol)	<i>Z_{dc}</i>
1	Streptomycin	0.67	0.56	-19.26	-0.95
2	Acarbose	0.64	0.60	—	-0.11
3	Cytarabine	0.64	0.56	-7.59	2.40
4	Streptozocin	0.63	0.72	-19.26	-0.69
5	Amikacin	0.63	0.59	—	-2.47
6	Fosdenopterin	0.63	0.56	-22.88	1.21
7	N-acetylglucosamine	0.61	0.57	-21.62	0.80
8	Oseltamivir	0.61	0.57	-24.69	-1.45
9	Plazomicin	0.61	0.59	—	-0.27
10	Peramivir	0.61	0.50	-18.90	—
11	Telbivudine	0.60	0.56	-8.05	—
12	Riboflavin	0.59	0.56	-14.98	0.12
13	Regadenoson	0.57	0.56	10.01	1.21
14	Ribavirin	0.54	0.57	10.85	-2.27
^a	Zanamivir	^a 1.00	0.77	-31.10	-0.93
^a	BCX-2798	0.77	^a 1.00	-23.05	—

^aRepresents the control, and *CE* is CDOCKER energy calculated by DS.

Additionally, the binding free energy for each frame trajectory in the last 10 ns (90–100 ns) of the MD simulation was computed using the MMPBSA.py script and the MMGBSA.py (Valdés-Tresanco et al., 2021). The total binding energy is denoted as ΔG , and the Equations 6–8 for calculating ΔG are as follows:

$$\Delta G_{\text{sol}} = \Delta G_{\text{NP}} + \Delta G_{\text{P}} \quad (6)$$

$$\Delta EMM = \Delta G_{\text{vdw}} + \Delta G_{\text{ele}} + \Delta G_{\text{int}} \quad (7)$$

$$\Delta G_{\text{TOTAL}} = \Delta G_{\text{sol}} + \Delta EMM \quad (8)$$

where ΔG_{sol} represents the solvation free energy and ΔEMM represents the gas phase energy. ΔEMM is also equal to the sum of van der Waals energy (ΔG_{vdw}), internal energy (ΔG_{int}), and electrostatic energy (ΔG_{ele}), whereas ΔG_{sol} is equal to the sum of polar solvation free energy (ΔG_{P}) and non-polar solvation free energy (ΔG_{NP}).

Results

Data collection

In this research, 2,585 approved drugs were obtained from the DrugBank database (see Supplementary Table S1A) as candidates. Subsequently, the chemical similarity between the controls (zanamivir and BCX-2798) and the 2,585 candidates were calculated, respectively. The results are listed in Supplementary Table S1B, C. At the same time, 324 PIV3 targets were compiled from the GeneCards, OMIM, and DisGeNET databases (see Supplementary Table S2).

Multi-similarity analysis

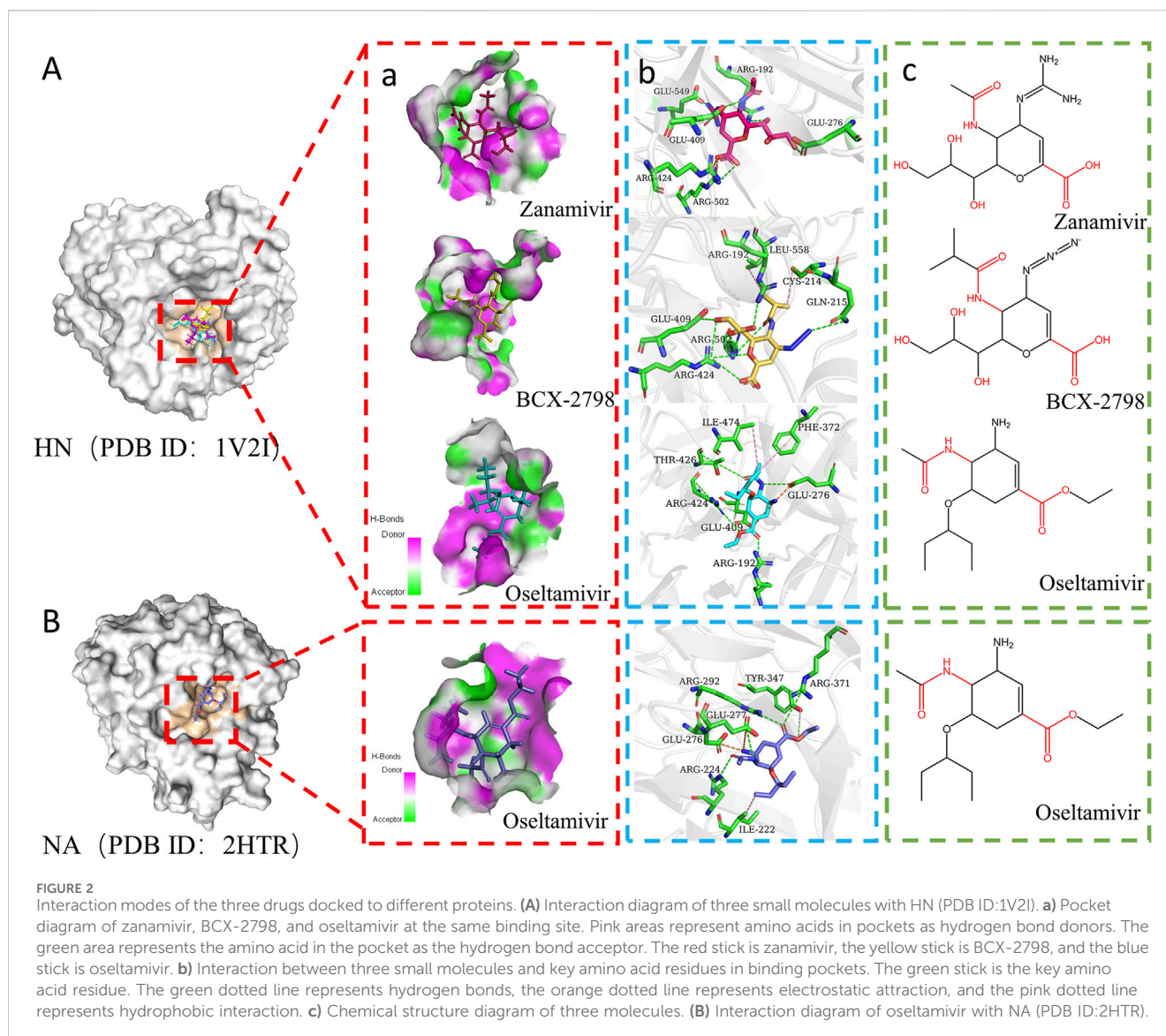
First, we calculated the semantic similarity of 1,364 diseases to PIV3 (see Supplementary Table S3). Only three diseases were identified with an $S > 0.5$ to PIV3, including respiratory syncytial virus (RSV) ($S = 0.78$), Ebola virus ($S = 0.55$), and Orthomyxoviridae ($S = 0.51$). Till now, to treat these three diseases, there were only four clinically approved drugs, which are zanamivir, oseltamivir, ribavirin, and peramivir.

After the chemical similarity of 2,585 candidates to the two controls were calculated, it was found that only 12 drugs had $T > 0.50$, as shown in Table 1 and Supplementary Figure S1. It means that only 12 drugs had higher structure similarity to the controls. From Table 1, the chemical similarity between zanamivir and BCX-2798 is significant ($T = 0.77$). When we observed their molecular structures, in Supplementary Figure S1, it was noticed that they share the same pyranic acid core, polyhydroxy side chain, and amide side chain. Similar to the control, most of the screened drugs contain oxygen-containing hexatomic rings, carboxyl groups, and amide structures. These functional groups may serve as crucial structures for inhibiting the activity of PIV3 and warrant further exploration.

Therefore, because two of the four candidates belonged to the 12, there were 14 selected candidates based on disease similarity ($S_{(H,A)} > 0.5$) and chemical similarity ($T > 0.56$) (as shown in Table 1).

Drug candidates docking to HN

The 14 candidates were molecularly docked with HN (PDB ID: 1V2I), and their docking energy values are listed in Table 1. It was

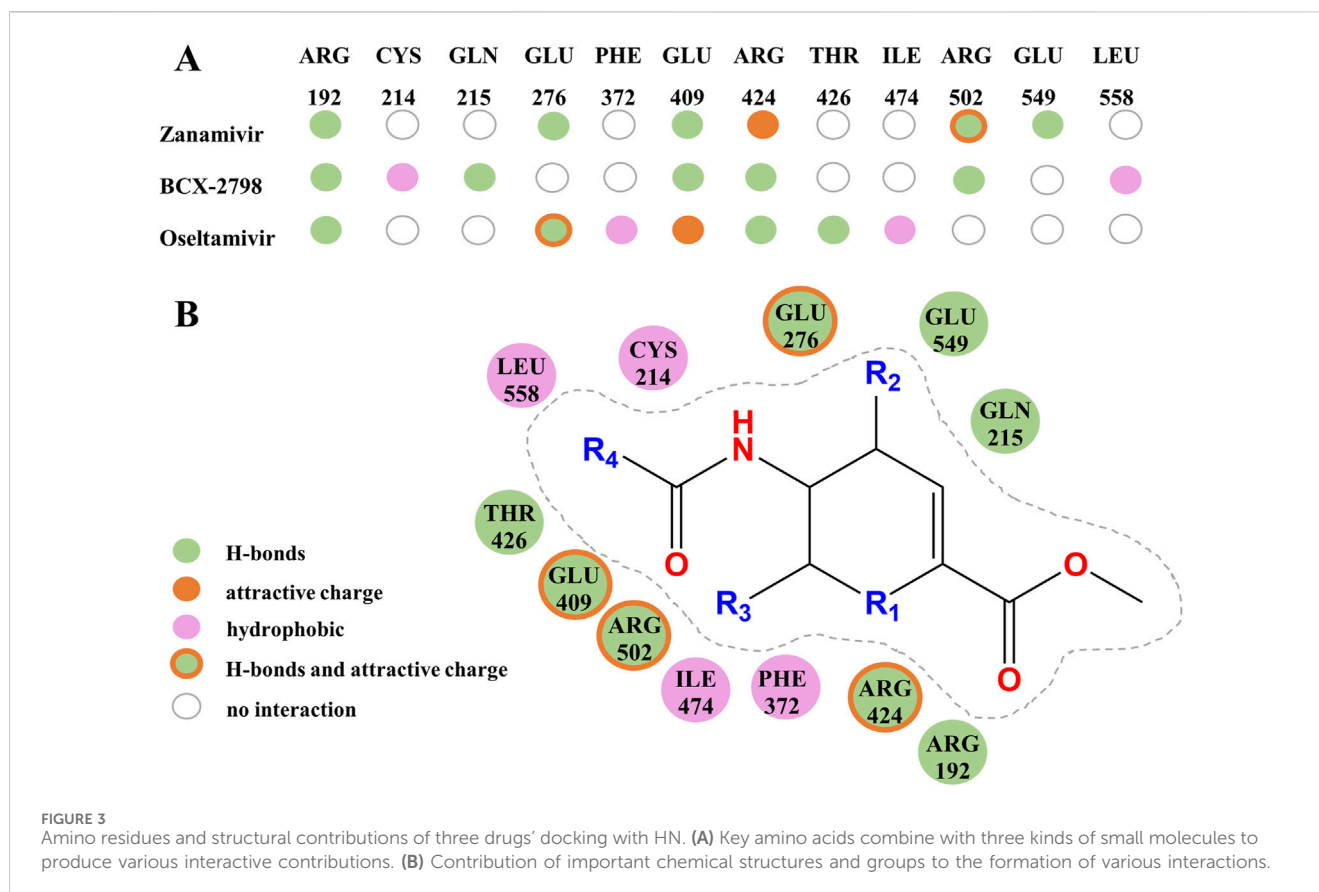


found that only oseltamivir ($CE = -24.69$ kcal/mol) had a lower docking energy value than BCX-2798 ($CE = -23.05$ kcal/mol), which indicated that oseltamivir bound to HN more stably than BCX-2798. Among all complexes, the top three drugs with stronger interactions were zanamivir, oseltamivir, and BCX-2798, so oseltamivir was the best among all the candidates. Visualization was carried out using DS 2019 and PyMol 2.5.0, as illustrated in Figure 2. We observed that all three compounds were stably bound to the pocket groove. Zanamivir was located in the shallow part of the binding pocket, revealing good flexibility and more options for binding poses. It was the same for BCX-2798. Oseltamivir occupied the deeper areas of the binding pocket, showing that oseltamivir had low flexibility, but it formed a more tightly bound complex. Oseltamivir was a good potential inhibitor of HN.

Furthermore, the intermolecular interactions of three complexes were observed and analyzed, and the contribution of key amino acid residues in binding pockets was explored Figures 2A, 3A. As shown in Figure 2A, in the three complexes, there were hydrogen bonding, electrostatic attraction, hydrophobic interaction, and some other

intermolecular forces between small-molecule compounds and key amino acid residues, which promoted the stability of intermolecular binding. Most of the hydrogen bonds and electrostatic attraction in the oseltamivir–HN complex were contributed by ARG and GLU residues, similar to the two control–HN complexes. Especially, the amino of oseltamivir was bound to GLU276, amide was bound to THR426, and carboxyl groups were bound to ARG192 and ARG424 of HN. Compared with the controls, since the alkylation of oseltamivir increased the hydrophobicity of the carboxyl side chain, it can be found that there were some π -alkyl interactions with ILE474 and PHE372 in oseltamivir, leading to more stable binding. Therefore, it can be concluded that oseltamivir has a strong bond–bond interaction with amino acids around the HN protein-binding pocket.

Oseltamivir was a successful classical drug designed case when it was considered a neuraminidase (NA) enzyme inhibitor in influenza viruses (Davies, 2010). Then, we compared the molecular docking results of oseltamivir and NA (PDB ID: 2HTR) (Russell et al., 2006) to explore the interaction between oseltamivir and PIV3. As shown



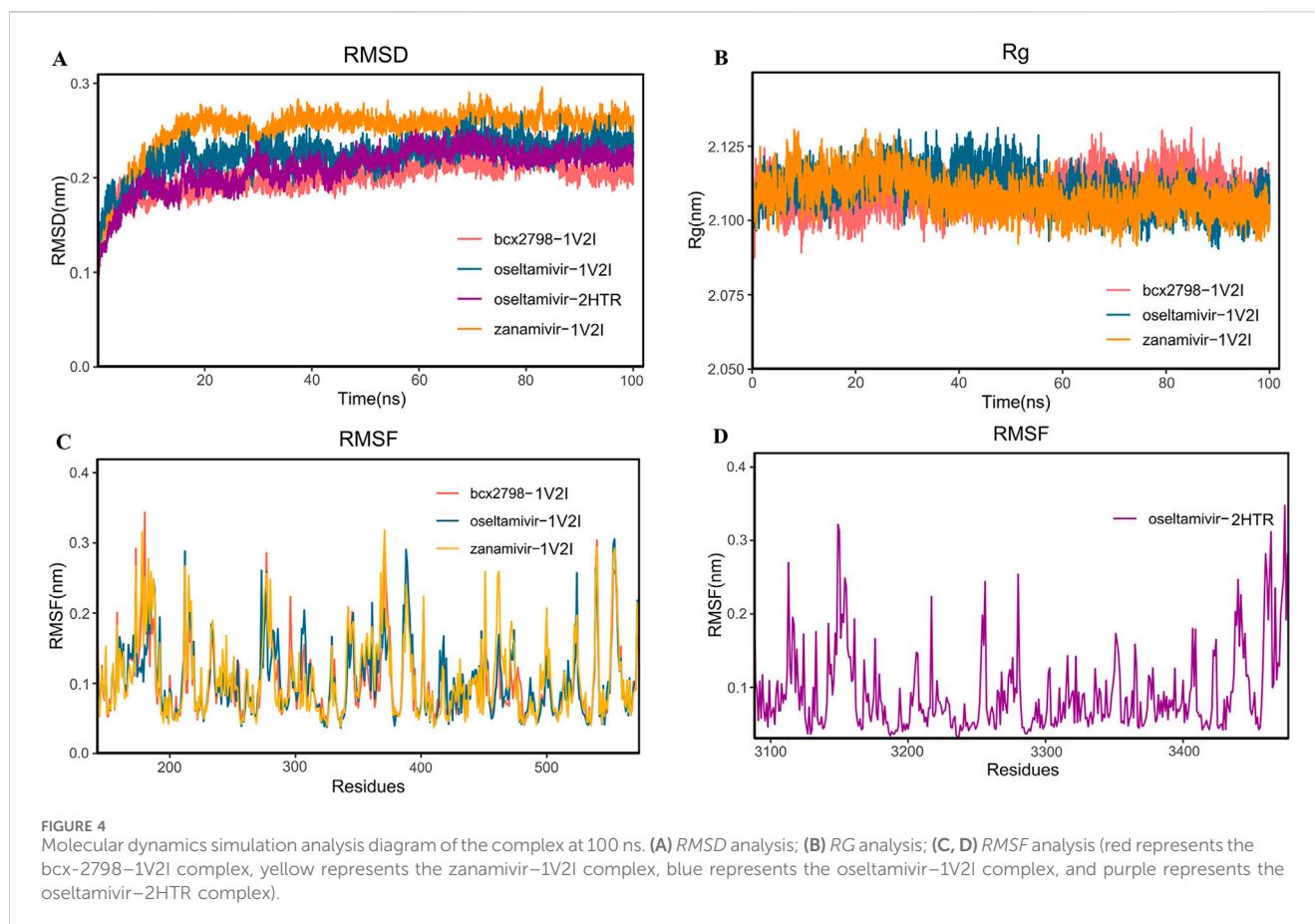
in Figure 2B, the side-chain amides, carboxyl groups, and amino groups of oseltamivir played crucial roles in inhibiting HN, similar to inhibiting NA (Laborda et al., 2016). Particularly, the acetamido fragment was well-accommodated within the cavity-binding domain both in HN and NA (Guillon et al., 2014). Thus, oseltamivir has the potential to inhibit PIV3.

Based on the contribution of amino residues binding to the pocket in Figure 3A and the common parent nucleus of three compounds (zanamivir, oseltamivir, and BCX-2798), the structural formula of potential lead compounds is derived, as shown in Figure 3B. From Figure 3B, the main structural differences among the three compounds are in R1, R2, R3, and R4. Among them, R1 mainly formed hydrogen bonds through residue binding, R2 formed hydrogen bonds and electrostatic interactions, and R3 and R4 could form hydrogen bonds and hydrophobic interactions with residues, respectively. From the analysis of the binding situation of the three molecules, for example, at the R1 position, BCX-2798 and zanamivir both have oxygen substitution groups, which can form a strong binding effect, while oseltamivir does not, indicating that the contribution to the binding energy here is little. R2 and R4 exhibited good binding affinity, in which the functional groups at the R2 position of the three drugs differed but all contained amines, and all substituted functional groups were alkyl at the R4 position. It indicated that R2 and R4 both made great contributions, but there were few differences among the three drugs. However, at the R3 position, they are all oxygen-substituted long-chain fatty acid groups with good binding affinity. However, it is an alkoxy group in oseltamivir,

while the others have hydroxyl groups, making it easy to form more hydrophobic interactions. This indicates that the contribution of this position is greater than that of R1 when the leading needs optimization for designing drugs. The side-chain amide and carboxyl groups of oseltamivir, along with the two controls, play a crucial role in facilitating complex binding. Various substituents (guanidine, azide, and amino) at the C4 position (R2) interact with crucial amino acids to facilitate intermolecular binding. As shown in Figure 3B, the guanidine group of zanamivir, the azide group of BCX-2798, and the amino group of oseltamivir are strongly bound to GLU549, GLN215, and GLU276 through hydrogen bonding or electrostatic interactions, respectively. In addition, as shown in Figure 2B, oseltamivir docks to neuraminidase (NA) at the amino acid residue that also binds to these key groups (amino, carboxyl, and amides). Thus, oseltamivir may be a good choice for anti-PIV3 treatment with good docking results.

Network proximity analysis of the candidates to PIV3

To further explore the potential candidates, we applied network proximity analysis to confirm it. A total of 324 disease targets were identified, with 314 targets prominently located in the PPI, to form the PIV3 disease module ($Z = 18.71$, $P < 0.0001$, randomly 1,000 times). In the PIV3 disease module, 231 targets formed the core disease module, and a total of 223 targets with $Z = 6.66$ and $p\text{-value} = 3.6 \times 10^{-10}$ formed the largest connected component



(LCC), as shown in [Supplementary Figure S2](#). It indicates that the localization of the LCC is significant in this disease module, which guarantees the formed PIV3 module is of good quality. Hence, network proximity analysis was based on this PIV3 disease module.

The targets of these 14 drugs were collected from the DrugBank and DGIdb databases to calculate network proximity (see [Supplementary Figure S4](#)). Then, the network proximity of the 14 candidates to the PIV3 disease module was calculated separately, and the results are also listed in [Table 1](#). Because BCX-2798 has not yet been approved for clinical use, the related targets have not yet been identified, and the drug targets of telbivudine and peramivir cannot be located in the PPI, only 12 candidates had Z_{dc} values. [Table 1](#) shows only four drugs, streptomycin, amikacin, oseltamivir, and ribavirin, with lower Z_{dc} than that of zanamivir (the control, $Z_{dc} = -0.93$). It means that these four drugs including oseltamivir were better candidates for anti-PIV3 treatment according to the network proximity analysis.

Molecular dynamics simulation analysis

Combining the above three screening methods, we arrived at the results, of which only oseltamivir met all the aforementioned anti-PIV3 drug screening requirements. We used *RMSD* to assess the binding stability of the complexes formed by oseltamivir, zanamivir, and BCX-2798 with 1V2I over a period of 100 ns. As shown in

[Figure 4A](#), the *RMSD* of the oseltamivir-1V2I complex gradually stabilized after 40 ns, and the average *RMSD* of the oseltamivir-1V2I complex (0.22 nm) was significantly lower than that of the zanamivir-1V2I complex (0.25 nm) in the control group, indicating that it exhibited better structural stability. All complexes including oseltamivir-1V2I demonstrate good structural stability.

To assess the compactness of the complex structure, the *RG* values were also calculated for the three above complexes and listed in [Figure 4B](#). As shown in [Figure 4B](#), each set of complexes remained significantly compact throughout the 100-ns simulation. The average *RGs* of the oseltamivir-1V2I complex and the two control complexes were the same, 2.11 nm. The oseltamivir-1V2I complex was similar to the two control complexes with a smaller *RG* in higher density, which led to a more stable system structure. As shown in [Figure 4C](#), the *RMSF* illustrates the flexibility of the molecule ([Awan et al., 2024](#)), and the average *RMSF* of zanamivir is 0.11 nm, while the mean *RMSFs* of both BCX-2798 and oseltamivir were 0.10 nm. Furthermore, in [Figure 4C](#), the three complexes show similar fluctuations in residue levels in different regions, leading to improved conformational optimization during substrate binding. Lower *RMSF* values may indicate active sites or binding sites, as these regions tend to become more stable after binding ligands. In oseltamivir-HN, the *RMSF* values of the key residues GLU276 (0.12 nm), GLU409 (0.13 nm), ARG424 (0.08 nm), THR426 (0.10 nm), and ARG502 (0.10 nm) at the

TABLE 2 Binding energies of three complexes (kcal/mol).

Parameters	Zanamivir	BCX-2798	Oseltamivir
MMPBSA			
ΔG_{vdw}	-32.95	-12.65	-20.70
ΔG_{ele}	-144.42	-83.30	-20.87
ΔG_p	163.58	86.40	35.16
ΔG_{NP}	-3.63	-1.98	-4.19
ΔG_{gas}	-177.37	-95.95	-41.57
ΔG_{sol}	159.95	84.43	30.97
ΔG_{TOTAL}	-17.42	-11.52	-10.60
MMGBSA			
ΔG_{vdw}	-33.17	-14.76	-21.42
ΔG_{ele}	-139.74	-93.21	-13.80
ΔG_p	154.27	94.82	24.82
ΔG_{NP}	-4.56	-2.55	-4.60
ΔG_{gas}	-172.92	-107.97	-35.22
ΔG_{sol}	149.70	92.27	20.22
ΔG_{TOTAL}	-23.21	-15.71	-15.00

binding pocket were very close to the average *RMSF* (0.10 nm), indicating that the binding between oseltamivir and the protein was relatively stable. Both the *RMSD* and *RG* of oseltamivir–HN indicate that the system is stable. The *RMSF* also shows stable residues near the ligand binding site, leading us to consider the complex binding to be stable.

Simultaneously, the binding free energies of the three complexes were calculated by using MM/PBSA and MM/GBSA, thereby determining the ligands' binding affinity at the protein active site (Bashir et al., 2023), and the results are shown in Table 2. The binding energy values obtained from the two algorithms are quite similar. The total binding free energies of oseltamivir–1V2I (-10.60 kcal/mol) and the two controls were less than -9.55 kcal/mol (normal threshold for strong binding), indicating strong binding ability for both compounds. Therefore, oseltamivir was a good candidate according to results of molecular dynamics simulation.

Discussion

In this article, we explored an integrated drug repurposing method, including disease similarity and chemical similarity as multi-similarity analysis approaches, molecular docking and molecular dynamic simulation methods as structure-based screening approaches, and network proximity analysis, in which we quantified the network distance between the disease module of PIV3 and the drug targets to probe the potential anti-PIV3 drugs. In addition, according to this drug repurposing protocol, we confirm that oseltamivir is the best potential anti-PIV3 drug.

In our research results, a similar pattern was observed when oseltamivir inhibited PIV3 and influenza A. As is known, zanamivir is a successful structural design drug for NA inhibitor, and oseltamivir is designed using zanamivir as the lead compound. Among them, the side-chain amides, carboxyl groups, and amino groups play a crucial role in inhibiting the influenza A virus (Laborda et al., 2016; Tao et al., 2022), and the acetamido fragment can be well-accommodated within the cavity-binding domain (Guillon et al., 2014). In our study, oseltamivir showed good chemical similarity to zanamivir and BCX-2798. Their shared side-chain amide and carboxyl group result in similar interactions when bound to HN using molecular docking, respectively. HN can accommodate larger acyl groups in the C5 binding region (Guillon et al., 2014), and the amides of all three complexes provide hydrogen bonds for protein binding. In the oseltamivir–HN complex, the amide also forms hydrogen bonds with THR426, which greatly contributes to the stable binding of the complex. This advantage distinguishes it from other complexes. The carboxylic acid side chain of oseltamivir forms hydrogen bonds with the surrounding arginine (ARG192 and ARG424), which enhances the binding stability between molecules.

Though some unique structures of oseltamivir can also facilitate its binding to HN, various substituents at position C4 (e.g., guanidine, azido, amide, and amino group) can enter the cavity around the residue of the active site of PIV3, thereby inhibiting the activity of PIV3 (El-Deeb et al., 2014; Rota et al., 2023). Specifically, the guanidine group of zanamivir is tightly bound to the hydrogen bond of GLU549, and the azido group of BCX-2798 can form hydrogen bonds with GLN215. The addition of the azido group significantly inhibits the activity of PIV (Chibanga et al., 2019). The amino group at the C4 position of oseltamivir enhances the electron-donating capability of nitrogen ions. This enhancement allows for the formation of an electrostatic attraction with GLU276 and GLU409, thereby increasing the charge attraction and binding force between molecules. Esterification of the oseltamivir side-chain carboxyl group leads to the elongation of the backbone, enabling it to penetrate deeper into the grooves of the binding site, thereby increasing the tightness of the binding complex. Therefore, the utilization of the chemical similarity method can offer more effective information for the development of anti-PIV3 drugs. Additionally, employing molecular docking in conjunction with molecular dynamics simulation methods can enhance the exploration of the structural interactions.

Searching for drugs based solely on chemical structure makes it difficult to consider the genetic regulatory processes of the disease itself. The synergistic functions of a large number of genes during disease initiation and progression were considered in this study. The association between PIV3 and oseltamivir based on genes was explored using network proximity analysis. The proximity can also be used to define the similarity between two drug candidates and covered several drug–disease associations. If a drug is proximal to the PIV3 disease, it is more likely to be effective than a distant drug. It indicated that the oseltamivir targets are more closely linked to the PIV3 disease module than those of the control (zanamivir). The network proximity of candidate targets to the PIV3 disease genes provides special insights into the candidate mechanism of action, uncovering the patho-biological components targeted by

candidates, and improves the feasibility and interpretability for drug repurposing.

However, if some drugs cannot be localized within the PPI network due to the incomplete human interactome network, these drugs may not be screened by network proximity. Repurposed drugs may skip phase-I clinical trials, but they still need to undergo phase-II and phase-III trials to assess their efficacy against new diseases. Although there are some limitations to this study, this approach allows for the rapid identification of potential therapeutic agents to mitigate the effects of emerging epidemics.

While computational methods are robust, clinical data or experimental validation of oseltamivir's inhibitory effect on PIV3 would significantly strengthen the findings. The clinical data were collected from the Second Affiliated Hospital of Chongqing Medical University, the Third Affiliated Hospital of Chongqing Medical University, and the Children's Hospital of Chongqing Medical University by searching on Yidu Cloud (<https://www.yiducoud.com.cn/>, from January 2016 to June 2024). There were 539 PIV3 cases, including 479 cases of children and infants under 6 years of age, 14 cases of individuals aged 7–17 years, 18 cases of individuals over 60 years old, and only 28 adult cases. Till now, there were no clinically approved antiviral drugs for treating PIV3 infection. Among 539 PIV3 patients, most mainly received expectorant cough medicine and nebulizer therapy without antiviral treatment, 203 patients received ribavirin treatment, and 17 patients were treated with oseltamivir. Of those 17 patients who were administered off-label oseltamivir, the patients did not undergo further treatment according to the medical records. This suggests that oseltamivir has a certain efficacy in treating PIV3 in clinical settings, aligning with the findings of our result. Given that most PIV3-infected patients are children, ribavirin can lead to severe adverse clinical reactions such as hemolytic anemia and teratogenic mutations (Sinclair et al., 2017). Oseltamivir is deemed safe for children over 1 year of age as an influenza treatment and has been FDA-approved for infants and young children over 14 days old for enhanced safety (Malosh et al., 2018). Therefore, we recommend considering oseltamivir for clinical application.

Conclusion

Oseltamivir is screened as a potential anti-PIV3 drug through a variety of drug repurposing methods as it has been considered an effective drug in clinical off-label medications for anti-PIV3 treatment in some children's hospitals in recent years. Oseltamivir exhibited high similarity to potential PIV3 inhibitors (zanamivir and BCX-2798), demonstrated strong binding ability to the key target protein HN, and was closely related to the PIV3 disease module. Therefore, oseltamivir fulfilled all the screening requirements and emerged as the most effective anti-PIV3 drug. The molecular docking results revealed that oseltamivir and PIV3 were bound through hydrogen bonding, electrostatic attraction, and hydrophobic interactions. In particular, the amides, carboxyl, and amino groups in oseltamivir are important structures for inhibiting PIV3. This multi-similarity drug repurposing method will be a feasible reference for other disease and drug repurposing research.

Data availability statement

The original contributions presented in the study are included in the article/[supplementary material](#), further inquiries can be directed to the corresponding author.

Author contributions

XC: Data curation, Formal Analysis, Investigation, Methodology, Resources, Validation, Visualization, Writing – original draft, Writing–review and editing. BZ: Conceptualization, Validation, Writing–review and editing, Data curation. XJ: Data curation, Methodology, Writing–review and editing. HZ: Methodology, Formal Analysis, Software, Writing–review and editing. AY: Formal Analysis, Data curation, Investigation, Writing–review and editing. TZ: Formal Analysis, Funding acquisition, Methodology, Validation, Writing–review and editing. CZ: Formal Analysis, Methodology, Validation, Writing–review and editing. XL: Data curation, Resources, Writing–review and editing. YZ: Conceptualization, Funding acquisition, Methodology, Project administration, Supervision, Validation, Writing – original draft, Writing–review and editing.

Funding

The author(s) declare that financial support was received for the research, authorship, and/or publication of this article. This research was financially supported by the National Natural Science Foundation of China (Grant numbers: 22176020 and 32072262), the Graduate Research and Innovation Project of Chongqing Municipal Education Commission (CYS23357), the CQMU Program for Youth Innovation in Future Medicine (W0181), and the Intelligent Medicine Research Project of Chongqing Medical University (YJSZHYX202203).

Conflict of interest

The authors declare that the research was conducted in the absence of any commercial or financial relationships that could be construed as a potential conflict of interest.

Publisher's note

All claims expressed in this article are solely those of the authors and do not necessarily represent those of their affiliated organizations, or those of the publisher, the editors, and the reviewers. Any product that may be evaluated in this article, or claim that may be made by its manufacturer, is not guaranteed or endorsed by the publisher.

Supplementary material

The Supplementary Material for this article can be found online at: <https://www.frontiersin.org/articles/10.3389/fphar.2024.1428925/full#supplementary-material>

References

- Aggarwal, M., and Plemper, R. K. (2020). Structural insight into paramyxovirus and Pneumovirus entry inhibition. *Viruses* 12, 342. doi:10.3390/v12030342
- Alymova, I. V., Portner, A., Takimoto, T., Boyd, K. L., Babu, Y. S., and McCullers, J. A. (2005). The novel parainfluenza virus hemagglutinin-neuraminidase inhibitor BCX 2798 prevents lethal synergism between a paramyxovirus and Streptococcus pneumoniae. *Antimicrob. Agents Chemother.* 49, 398–405. doi:10.1128/AAC.49.1.398-405.2005
- Alymova, I. V., Taylor, G., Takimoto, T., Lin, T.-H., Chand, P., Babu, Y. S., et al. (2004). Efficacy of novel hemagglutinin-neuraminidase inhibitors BCX 2798 and BCX 2855 against human parainfluenza viruses *in vitro* and *in vivo*. *Antimicrob. Agents Chemother.* 48, 1495–1502. doi:10.1128/AAC.48.5.1495-1502.2004
- Awan, Z. A., Khan, H. A., Jamal, A., Shams, S., Zheng, G., Wadood, A., et al. (2024). *In silico* exploration of the potential inhibitory activities of in-house and ZINC database lead compounds against alpha-glucosidase using structure-based virtual screening and molecular dynamics simulation approach. *J. Biomol. Struct. Dyn.*, 1–11. doi:10.1080/07391102.2023.2298391
- Bailly, B., Dirr, L., El-Deeb, I. M., Altmeyer, R., Guillon, P., and von Itzstein, M. (2016). A dual drug regimen synergistically blocks human parainfluenza virus infection. *Sci. Rep.* 6, 24138. doi:10.1038/srep24138
- Bashir, Y., Noor, F., Ahmad, S., Tariq, M. H., Qasim, M., Tahir Ul Qamar, M., et al. (2023). Integrated virtual screening and molecular dynamics simulation approaches revealed potential natural inhibitors for DNMT1 as therapeutic solution for triple negative breast cancer. *J. Biomol. Struct. Dyn.* 42, 1099–1109. doi:10.1080/07391102.2023.2198017
- Bhasin, S., Nadar, M., and Hasija, Y. (2022). Epicatechin analogues may hinder human parainfluenza virus infection by inhibition of hemagglutinin neuraminidase protein and prevention of cellular entry. *J. Mol. Model* 28, 319. doi:10.1007/s00894-022-05310-9
- Branche, A. R., and Falsey, A. R. (2016). Parainfluenza virus infection. *Semin. Respir. Crit. Care Med.* 37, 538–554. doi:10.1055/s-0036-1584798
- Chibanga, V. P., Dirr, L., Guillon, P., El-Deeb, I. M., Bailly, B., Thomson, R. J., et al. (2019). New antiviral approaches for human parainfluenza: inhibiting the haemagglutinin-neuraminidase. *Antivir. Res.* 167, 89–97. doi:10.1016/j.antiviral.2019.04.001
- Contreras, E. M., Monreal, I. A., Ruvalcaba, M., Ortega, V., and Aguilar, H. C. (2021). Antivirals targeting paramyxovirus membrane fusion. *Curr. Opin. Virol.* 51, 34–47. doi:10.1016/j.coviro.2021.09.003
- Dai, W., Tang, T., Dai, Z., Shi, D., Mo, L., and Zhang, Y. (2020). Probing the mechanism of hepatotoxicity of hexabromocyclododecanes through toxicological network analysis. *Environ. Sci. Technol.* 54, 15235–15245. doi:10.1021/acs.est.0c03998
- Darden, T., York, D., and Pedersen, L. (1993). Particle mesh Ewald: an N log(N) method for Ewald sums in large systems. *J. Chem. Phys.* 98, 10089–10092. doi:10.1063/1.464397.[CrossRef Exact] [CS: 100]Refstyled
- Davies, B. E. (2010). Pharmacokinetics of oseltamivir: an oral antiviral for the treatment and prophylaxis of influenza in diverse populations. *J. Antimicrob. Chemother.* 65 (Suppl. 2), ii5–ii10. doi:10.1093/jac/dkq015
- Durai, P., Ko, Y.-J., Pan, C.-H., and Park, K. (2020). Evolutionary chemical binding similarity approach integrated with 3D-QSAR method for effective virtual screening. *BMC Bioinforma.* 21, 309. doi:10.1186/s12859-020-03643-x
- El-Deeb, I. M., Guillon, P., Winger, M., Eveno, T., Haselhorst, T., Dyason, J. C., et al. (2014). Exploring human parainfluenza virus type-1 hemagglutinin-neuraminidase as a target for inhibitor discovery. *J. Med. Chem.* 57, 7613–7623. doi:10.1021/jm500759v
- Gu, R.-X., Liu, L. A., Wei, D.-Q., Du, J.-G., Liu, L., and Liu, H. (2011). Free energy calculations on the two drug binding sites in the M2 proton channel. *J. Am. Chem. Soc.* 133, 10817–10825. doi:10.1021/ja1114198
- Guillon, P., Dirr, L., El-Deeb, I. M., Winger, M., Bailly, B., Haselhorst, T., et al. (2014). Structure-guided discovery of potent and dual-acting human parainfluenza virus haemagglutinin-neuraminidase inhibitors. *Nat. Commun.* 5, 5268. doi:10.1038/ncomms6268
- Guney, E., Menche, J., Vidal, M., and Barabasi, A.-L. (2016). Network-based *in silico* drug efficacy screening. *Nat. Commun.* 7, 10331. doi:10.1038/ncomms10331
- Indumathi, C. P., Bupesh, G., Vasanth, S., Senthilkumar, V., Anandh, A. V., and Pandian, K. (2019). Molecular docking analysis of zanamavir with haem agglutinin neuraminidase of human para influenza virus type 3. *Bioinformatics* 15, 730–734. doi:10.6026/97320630015730
- Khan, A., Adil, S., Qudisia, H. A., Waheed, Y., Alshabrimi, F. M., and Wei, D.-Q. (2023). Structure-based design of promising natural products to inhibit thymidylate kinase from Monkeypox virus and validation using free energy calculations. *Comput. Biol. Med.* 158, 106797. doi:10.1016/j.combiomed.2023.106797
- Koulig, S., Jani, V., Uppuladinne, M., Sonavane, U., Nath, A. K., Darbari, H., et al. (2021). Drug repurposing studies targeting SARS-CoV-2: an ensemble docking approach on drug target 3C-like protease (3CLpro). *J. Biomol. Struct. Dyn.* 39, 5735–5755. doi:10.1080/07391102.2020.1792344
- Kumar, R., Kumar, V., and Lee, K. W. (2021). A computational drug repurposing approach in identifying the cephalosporin antibiotic and anti-hepatitis C drug derivatives for COVID-19 treatment. *Comput. Biol. Med.* 130, 104186. doi:10.1016/j.combiomed.2020.104186
- Laborda, P., Wang, S.-Y., and Voglmeir, J. (2016). Influenza neuraminidase inhibitors: synthetic approaches, derivatives and biological activity. *Molecules* 21, 1513. doi:10.3390/molecules21111513
- Lawrence, M. C., Borg, N. A., Streltsov, V. A., Pilling, P. A., Epa, V. C., Varghese, J. N., et al. (2004). Structure of the haemagglutinin-neuraminidase from human parainfluenza virus type III. *J. Mol. Biol.* 335, 1343–1357. doi:10.1016/j.jmb.2003.11.032
- Li, H., Fan, J., Vitali, F., Berghout, J., Aberasturi, D., Li, J., et al. (2018). Novel disease syndromes unveiled by integrative multiscale network analysis of diseases sharing molecular effectors and comorbidities. *BMC Med. Genomics* 11, 112. doi:10.1186/s12920-018-0428-9
- Malosh, R. E., Martin, E. T., Heikkinen, T., Brooks, W. A., Whitley, R. J., and Monto, A. S. (2018). Efficacy and safety of oseltamivir in children: systematic review and individual patient data meta-analysis of randomized controlled trials. *Clin. Infect. Dis.* 66, 1492–1500. doi:10.1093/cid/cix1040
- Menche, J., Sharma, A., Kitsak, M., Ghiassian, S. D., Vidal, M., Loscalzo, J., et al. (2015). Disease networks. Uncovering disease-disease relationships through the incomplete interactome. *Science* 347, 1257601. doi:10.1126/science.1257601
- Mizuta, K., Tsukagoshi, H., Ikeda, T., Aoki, Y., Abiko, C., Itagaki, T., et al. (2014). Molecular evolution of the haemagglutinin-neuraminidase gene in human parainfluenza virus type 3 isolates from children with acute respiratory illness in Yamagata prefecture, Japan. *J. Med. Microbiol.* 63, 570–577. doi:10.1099/jmm.0.068189-0
- Morselli Gysi, D., do Valle, F., Zitnik, M., Ameli, A., Gan, X., Varol, O., et al. (2021). Network medicine framework for identifying drug-repurposing opportunities for COVID-19. *Proc. Natl. Acad. Sci. U. S. A.* 118, e2025581118. doi:10.1073/pnas.2025581118
- Moscona, A. (2005). Entry of parainfluenza virus into cells as a target for interrupting childhood respiratory disease. *J. Clin. Invest.* 115, 1688–1698. doi:10.1172/JCI25669
- Nayar, D., Agarwal, M., and Chakravarty, C. (2011). Comparison of tetrahedral order, liquid state anomalies, and hydration behavior of mTIP3P and TIP4P water models. *J. Chem. Theory Comput.* 7, 3354–3367. doi:10.1021/ct2002732
- Palmer, S. G., DeVito, I., Jenkins, S. G., Niewiesk, S., Porotto, M., and Moscona, A. (2014). Circulating clinical strains of human parainfluenza virus reveal viral entry requirements for *in vivo* infection. *J. Virol.* 88, 13495–13502. doi:10.1128/JVI.101965-14
- Parihar, A., Sonia, Z. F., Akter, F., Ali, M. A., Hakim, F. T., and Hossain, M. S. (2022). Phytochemicals-based targeting RdRp and main protease of SARS-CoV-2 using docking and steered molecular dynamic simulation: a promising therapeutic approach for Tackling COVID-19. *Comput. Biol. Med.* 145, 105468. doi:10.1016/j.combiomed.2022.105468
- Pushpakom, S., Iorio, F., Eyers, P. A., Escott, K. J., Hopper, S., Wells, A., et al. (2019). Drug repurposing: progress, challenges and recommendations. *Nat. Rev. Drug Discov.* 18, 41–58. doi:10.1038/nrd.2018.168
- Rafeek, R. A. M., Divarathna, M. V. M., and Noordeen, F. (2021). A review on disease burden and epidemiology of childhood parainfluenza virus infections in Asian countries. *Rev. Med. Virol.* 31, e2164. doi:10.1002/rmv.2164
- Rota, P., La Rocca, P., Bonfante, F., Pagliari, M., Piccoli, M., Cirillo, F., et al. (2023). Design, synthesis, and antiviral evaluation of sialic acid derivatives as inhibitors of newcastle disease virus hemagglutinin-neuraminidase: a translational study on human parainfluenza viruses. *ACS Infect. Dis.* 9, 617–630. doi:10.1021/acscinfedis.2c00576
- Russell, R. J., Haire, L. F., Stevens, D. J., Collins, P. J., Lin, Y. P., Blackburn, G. M., et al. (2006). The structure of H5N1 avian influenza neuraminidase suggests new opportunities for drug design. *Nature* 443, 45–49. doi:10.1038/nature05114
- Schmidt, A. C., Schaap-Nutt, A., Bartlett, E. J., Schomacker, H., Boonyaratankornkit, J., Karron, R. A., et al. (2011). Progress in the development of human parainfluenza virus vaccines. *Expert Rev. Respir. Med.* 5, 515–526. doi:10.1586/ers.11.32
- Sinclair, S. M., Jones, J. K., Miller, R. K., Greene, M. F., Kwo, P. Y., and Maddrey, W. C. (2017). The ribavirin pregnancy registry: an interim analysis of potential teratogenicity at the mid-point of enrollment. *Drug Saf.* 40, 1205–1218. doi:10.1007/s40264-017-0566-6
- Sonkar, C., Doharey, P. K., Rathore, A. S., Singh, V., Kashyap, D., Sahoo, A. K., et al. (2021). Repurposing of gastric cancer drugs against COVID-19. *Comput. Biol. Med.* 137, 104826. doi:10.1016/j.combiomed.2021.104826
- Tang, T., Gan, X., Zhou, L., Pu, K., Wang, H., Dai, W., et al. (2023). Exploring the hepatotoxicity of drugs through machine learning and Network toxicological methods. *CBIO* 18, 484–496. doi:10.2174/1574893618666230316122534
- Tao, J., Wang, H., Wang, W., Mi, N., Zhang, W., Wen, Q., et al. (2022). Binding mechanism of oseltamivir and influenza neuraminidase suggests perspectives for the design of new anti-influenza drugs. *PLoS Comput. Biol.* 18, e1010343. doi:10.1371/journal.pcbi.1010343

- Tayubi, I. A., and Madar, I. H. (2023). Identification of potential inhibitor targeting KRAS mutation in Papillary Thyroid Carcinoma through molecular docking and dynamic simulation analysis. *Comput. Biol. Med.* 152, 106377. doi:10.1016/j.combiomed.2022.106377
- Valdés-Tresanco, M. S., Valdés-Tresanco, M. E., Valiente, P. A., and Moreno, E. (2021). gmx_MMPBSA: a new tool to perform end-state free energy calculations with GROMACS. *J. Chem. Theory Comput.* 17, 6281–6291. doi:10.1021/acs.jctc.1c00645
- Van Den Bergh, A., Bailly, B., Guillon, P., von Itzstein, M., and Dirr, L. (2022). Antiviral strategies against human metapneumovirus: targeting the fusion protein. *Antivir. Res.* 207, 105405. doi:10.1016/j.antiviral.2022.105405
- Wang, H., Zhang, J., Lu, Z., Dai, W., Ma, C., Xiang, Y., et al. (2022). Identification of potential therapeutic targets and mechanisms of COVID-19 through network analysis and screening of chemicals and herbal ingredients. *Brief. Bioinform* 23, bbab373. doi:10.1093/bib/bbab373
- Wang, J. Z., Du, Z., Payattakool, R., Yu, P. S., and Chen, C.-F. (2007). A new method to measure the semantic similarity of GO terms. *Bioinformatics* 23, 1274–1281. doi:10.1093/bioinformatics/btm087
- Wang, Y., Yang, H., Chen, L., Jafari, M., and Tang, J. (2021). Network-based modeling of herb combinations in traditional Chinese medicine. *Brief. Bioinform* 22, bbab106. doi:10.1093/bib/bbab106
- Xi, K., Zhang, M., Li, M., Tang, Q., Zhao, Q., and Chen, W. (2023). Unveiling the mechanisms of nephrotoxicity caused by nephrotoxic compounds using toxicological network analysis. *Mol. Ther. Nucleic Acids* 34, 102075. doi:10.1016/j.omtn.2023.102075
- Yap, C. W. (2011). PaDEL-descriptor: an open source software to calculate molecular descriptors and fingerprints. *J. Comput. Chem.* 32, 1466–1474. doi:10.1002/jcc.21707
- Yildirim, M. A., Goh, K.-I., Cusick, M. E., Barabási, A.-L., and Vidal, M. (2007). Drug-target network. *Nat. Biotechnol.* 25, 1119–1126. doi:10.1038/nbt1338
- Yin, Z., Liu, S., Yang, X., Chen, M., Du, J., Liu, H., et al. (2023). LSD1-Based reversible inhibitors virtual screening and binding mechanism computational study. *Molecules* 28, 5315. doi:10.3390/molecules28145315
- Zhou, Y., Hou, Y., Shen, J., Huang, Y., Martin, W., and Cheng, F. (2020). Network-based drug repurposing for novel coronavirus 2019-nCoV/SARS-CoV-2. *Cell Discov.* 6, 14. doi:10.1038/s41421-020-0153-3